# Variable cavity volume tooling for high-performance resin infusion moulding

**G J Gibbons***, **J J Segui-Garza,** and **R G Hansell**
School of Engineering, University of Warwick, Coventry, UK

*The manuscript was received on 7 April 2009 and was accepted after revision for publication on 17 November 2009.*

DOI: 10.1243/09544100JAERO582

**Abstract:** This article describes the research carried out by Warwick under the BAE Systems/EPSRC programme 'Flapless Aerial Vehicles Integrated Interdisciplinary Research – FLAVIIR'. Warwick's aim in FLAVIIR was to develop low-cost innovative tooling technologies to enable the affordable manufacture of complex composite aerospace structures and to help realize the aim of the Grand Challenge of maintenance-free, low-cost unmanned aerial vehicle manufacture. This article focuses on the evaluation of a novel tooling process (variable cavity tooling) to enable the complete infusion of resin throughout non-crimp fabric within a mould cavity under low (0.1 MPa) injection pressure. The contribution of the primary processing parameters to the mechanical properties of a carbon composite component (bulk-head lug section), and the interactions between parameters, was determined. The initial mould gap ($d_i$) was identified as having the most significant effect on all measured mechanical properties, but complex interactions between $d_i$, $n$ (number of fabric layers), and $v_c$ (mould closure rate) were observed. The process capability was low due to the manual processing, but was improved through process optimization, and delivered properties comparable to high-pressure resin transfer moulding.

**Keywords:** resin transfer moulding, tooling, carbon fibre composite

## 1 INTRODUCTION

Unmanned aerial vehicles (UAVs) are becoming increasingly important to the UK defence sector as they provide a means of both gathering reconnaissance and deploying loads over a hostile theatre without risking loss of life or expensive hardware. The requirement for low cost is thus paramount and this has forced some of the key suppliers to identify new low-cost manufacturing processes to deliver the UAVs of the future.

To address this need, EPSRC and BAE Systems initiated the Flapless Aerial Vehicles Integrated Interdisciplinary Research (FLAVIIR) project, in collaboration with key centres of research excellence within the UK academic community. FLAVIIR is a multi-disciplinary, integrated research project, aimed at developing innovative technologies for the low-cost manufacture of next-generation UAVs, with a focus on delivering maintenance-free, low-cost airframes. To achieve high levels of reliability, and zero or low-maintenance effort, these vehicles will be predominantly carbon fibre composite (CFC) based. Since reconfigurable UAVs are envisaged, potentially some parts will be only manufactured in low volumes, and the high tooling costs associated with traditional resin transfer mould (RTM) tooling would make the UAVs prohibitively expensive to manufacture, and would stifle the development of next-generation UAVs, which would have a negative effect on the economy and security of the UK.

Warwick's Rapid Prototyping & Tooling Centre (RP&M), located within WMG, University of Warwick, was chosen as an Academic Capability Partner to BAE Systems, charged with developing innovative tooling technologies to enable the affordable manufacture of complex composite aerospace structures. Within that remit, a focus of Warwick's research was investigation into methodologies and technologies to deliver improvements in material properties (tensile and flexural strength) of CFC components when processed using dry fabrics under low-pressure resin infusion, which would traditionally not deliver the strength and quality requirements demanded by the aerospace

*Corresponding author: School of Engineering, University of Warwick, Coventry CV4 7AL, UK.
email: g.j.gibbons@warwick.ac.uk

sector, since low-pressure injection of large components would be susceptible to higher void contents [**1**], resulting in lower strength [**2**].

Closed-mould RTM is an important processing technology for composites manufacture that has found wide application in a wide range of sectors, including aerospace and defence [**3**–**6**], automotive parts [**7**, **8**], power generation [**9**], and other cost-sensitive applications. RTM has many advantages, including relatively short cycle time [**10**] and low volatile emissions [**10**, **11**], and provides high-quality components [**12**]. Despite these many advantages, RTM has significant limitations for the manufacture of large-scale components requiring a high fibre content for high strength applications (volume fraction of 55–60 per cent). Owing to the increased pressure gradient over long distances and the low permeability of dense fibre reinforcements [**11**, **13**], the infusion of large components is excessively slow, and can lead to components with high void contents [**1**], which can reduce the strength of the composite, and particularly the interlaminar shear strength [**2**]. The use of higher resin injection pressures and multiple inlet ports has been investigated to achieve higher infusion rates [**11**, **14**], although higher flowrates can result in movement of the fabric 'fabric wash' and deformation of the fabric structure [**15**]. A number of process modifications have attempted to mitigate this problem, including Seeman composite resin infusion moulding (SCRIMP) [**16**] and vacuum-assisted RTM (VARTM) [**17**, **18**], both of which employ a resin porous layer to encourage resin flow longitudinally over the component area. Although successful to some degree in improving resin infusion rates, the rates are still limited by the permeability of the fabric, the viscosity of the resin, and the injection pressure, but, most importantly, SCRIMP and VARTM are single-sided mould processes, and as such are incapable of providing two high-quality surfaces, and cannot achieve the degree of the fibre consolidation possible with closed-mould RTM.

The use of 'active' or articulated cavities in closed-mould RTM has been investigated as a means of applying a mechanical pressure to the resin so as to induce a local high-pressure gradient at positions remote from the injection port. Ikegawa *et al.* [**10**] employed a moveable mould half that was lowered down onto the fibre after injection to provide a compressive squeezing force onto the resin, thus increasing infusion rates. The primary aim of the research, however, was to achieve lower void fractions than previously obtained using RTM, which it was successful in delivering. It was concluded that the fabric permeability was increased by higher resin flowrates, thus preventing the formation of voids through air entrapment. Despite this, however, a minimum void volume fraction of approximately 3 per cent was only achievable. Choi and Dharan [**11**] took a similar but significantly more complex approach, using a set of adjacent moveable core blocks. Resin compression and infusion was delivered through sequential raising and lowering of the blocks to transfer the resin load longitudinally through the fibre. This research demonstrated significant resin infusion rate increases over standard RTM but no results were presented for the resulting mechanical properties of the component so formed. Furthermore, the mould tool was very complex and would be extremely expensive to manufacture, and would be likely not to be economically feasible for the manufacture of low-cost UAVs.

From the industrial requirements (two high-quality surfaces, high fibre content (55–60 per cent), low void fraction, and low-cost), and with consideration of the previous research, the primary characteristics of an ideal forming process were proposed.

1. Closed-mould process, providing good levels of consolidation.

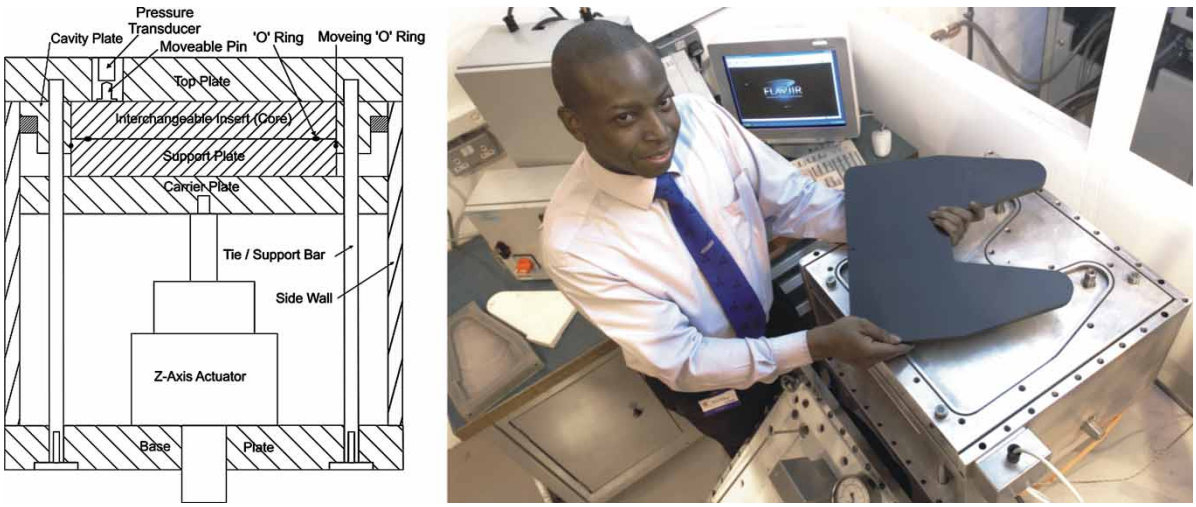


**Fig. 1** Diagrammatic representation of the tool and the manufactured tool and bulk-head test part

2. Allows vacuum application to remove entrapped air prior to resin infusion.
3. Allows easy infusion of resin.
4. Low cost.

## 2 METHODOLOGY

The approach taken in FLAVIIR aimed to address these four fundamental requirements. The development (variable cavity tooling – VCT) employs the principle of Ikegawa *et al.* [**10**], in that the tool core is moved after resin infusion, but overcomes the limitations of the previous research, where minimum porosity levels of 2–3 per cent were observed, by sealing the cavity prior to infusion, thus facilitating evacuation of the entrapped air, and maintaining this seal during cavity closure and the infusion stages. Furthermore, the work advances over the prior published work through a statistical analysis of the process, providing process parameters – property relationships and process capability.

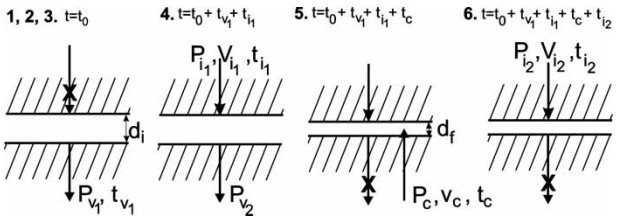


**Fig. 2** Diagrammatic representation of the sample manufacturing process

**Table 1** Material properties for the tri-axial MCX 1181270 CFC fabric

| Layer | AF | Fibre | Nominal weight (gsm) | Tolerance (gsm) |
|---|---|---|---|---|
| 0° | 077 | STS5631 24 K | 376 | ±5 |
| +45° | 077 | STS5631 24 K | 188 | ±5 |
| −45° | 077 | STS5631 24 K | 188 | ±5 |

### 2.1 Tool manufacture

A tool was designed and manufactured within the RP&M group. Since the tool was to be employed for low-pressure vacuum-assisted RTM (VARTM), the tool was designed to operate at injection pressures up to 0.2 MPa and was constructed from 2014 aluminium to minimize cost. Although the aim of this article is not to provide a cost analysis of the process, cost improvement over traditional processing may be inferred through the use of lower-cost tooling materials, and the processing of lower-cost non-woven fabrics. The tool was designed to manufacture a full-size section of the bulk-head component, which was a standard test component used for material validation in the low-cost materials development area of FLAVIIR. Figure 1 shows the tool and a diagrammatic drawing of the tool. Cavity movement was performed using

**Table 2** A description of the process parameters employed and their nominal values

| Stage | Parameter | Description | Value |
|---|---|---|---|
| 1 | *Load CFC laminates into cavity* | | |
| | $n$ | Number of CFC fabric layers | 6, 7, 8* |
| 2 | *Close tool cavity to initial tool gap* | | |
| | $d_i$ | Initial mould gap | 6, 7, 8 mm* |
| 3 | *Removal of entrapped gas, resin input closed* | | |
| | $t_o$ | Initial time | 0 s |
| | $P_{v1}$ | Vacuum pressure | −0.1 MPa |
| | $t_{v1}$ | Application time of $P_{v1}$ | 600 s |
| 4 | *Resin injection* | | |
| | $t_{i1}$ | Time of application of resin injection pressure | ∼10 min, until resin flow from vacuum port slowed down significantly |
| | $P_{i1}$ | Resin injection pressure | 0.1 MPa |
| | $V_{i1}$ | Resin volume | Dependent on $T_i$, ∼500 mm$^3$ |
| | $P_{v2}$ | Vacuum pressure during resin injection | −0.1 MPa |
| 5 | *Mould closure to final height* | | |
| | $P_c$ | Closure pressure | Measured value |
| | $v_c$ | Mould cavity closure rate | 0.25, 0.5, 1 mm/min[a] |
| | $d_f$ | Final mould gap | 5 mm |
| | $t_c$ | Closure time | Dependent on $v_c$, $d_i$ |
| 6 | *Application of injection pressure after mould closure* | | |
| | $t_{i2}$ | Time of application of resin injection pressure after mould closure | 20–30 min, until resin gels |
| | $P_{i2}$ | Resin injection pressure | 0.1 MPa |

*Variable parameters employed in designed experimental research.

a 50 kN programmable logic control (PLC)-controlled $Z$-axis, sufficient to provide movement for a 0.2 MPa injection pressure. The cavity was sealed using a viton 'o' ring located around the periphery of the support plate. The tool was integrally heated using electrical heating elements embedded into the support and top plates, with proportional integral derivative (PID) control. Process monitoring was achieved using thermocouple temperature measurement (one in the top plate and one in the support plate) and cavity pressure measurement was achieved using a pressure transducer (−0.1 to 1 MPa), located in the top plate. To ensure the reliable, repeatable response of the transducer, resin pressure was transferred from the cavity to the transducer through a moveable pin, located in the cavity face of the top plate (Fig. 1).

### 2.2 Sample preparation

A tri-axial (−45,0,+45) dry non-crimp fabric (NCF) (MCX 1181270—Sigmatex UK Ltd, Runcorn, UK) was employed, the properties of which are given in Table 1.

Araldite LY3505 epoxy resin, using XB 3404 hardener (Huntsman Advanced Materials (Europe) BVBA, Belgium), was employed as the resin matrix. A resin to hardener matrix of 3:1 was employed. The following is the experimental process for the manufacture of a test sample.

1. Load CFC laminates into a cavity.
2. Close the cavity to initial gap.
3. Evacuate the entrapped air using vacuum.
4. Inject the resin while maintaining vacuum.
5. Close the mould cavity to final height when resin flow appears in the vacuum port.
6. Apply injection pressure until gellation of resin occurs.
7. Close off the vacuum port.
8. Heat cure the resin for 10 h at 60 °C.

The stages up to resin gellation (stages 1–6) are represented diagrammatically (Fig. 2), with the parameters employed in each stage summarized in Table 2.

The research aim was to investigate the effect of initial cavity volume, cavity closure rate, and volume of CFC fibre on the quality (tensile, flexural properties, and density) of the components. The variable parameters indicated in Table 2 ($d_i$, $n$, and $v_c$) were chosen as the independent variables. A design of experiment (DoE) methodology (three-parameter,

**Table 3** Experimental parameter matrix populated with experimental process parameters

| Run | $d_i$ (mm) | $n$ | $v_c$ (mm/min) | Run | $d_i$ (mm) | $n$ | $v_c$ (mm/min) |
|---|---|---|---|---|---|---|---|
| 1 | 6 | 6 | 0.25 | 9 | 7 | 7 | 0.5 |
| 2 | 6 | 6 | 1 | 10 | 6 | 7 | 0.5 |
| 3 | 6 | 8 | 0.25 | 11 | 8 | 7 | 0.5 |
| 4 | 6 | 8 | 1 | 12 | 7 | 6 | 0.5 |
| 5 | 8 | 6 | 0.25 | 13 | 7 | 8 | 0.5 |
| 6 | 8 | 6 | 1 | 14 | 7 | 7 | 0.25 |
| 7 | 8 | 8 | 0.25 | 15 | 7 | 7 | 1 |
| 8 | 8 | 8 | 1 | | | | |

**Fig. 3** Dominant failure modes for the tensile testing of laminates. LHS/RHS: explosive gage middle; centre: long splitting gage middle


**Fig. 4** The dominant failure modes for the flexural testing of laminates. LHS: single laminar failure; RHS: multiple laminar failure

three-level, central composite design with one centre point and six repetitions) was chosen to enable an investigation of the significance and independence of each of these parameters on sample quality. The experimental parameter matrix is given in Table 3.

From the results of a statistical analysis and optimization of the samples manufactured (given in section 3.2), a confirmation run was performed using the optimized parameters for $E_b$ and $\sigma_f$. The sample was manufactured using the process described above.

### 2.3 Sample evaluation

The samples were investigated mechanically. Tensile and flexural strengths and moduli were evaluated using the sample and test specifications described in EN ISO 527_4:1997 [**19**] EN ISO 14125:1998 [**20**], respectively. Six samples for tensile flexural were prepared for each of the runs (including the confirmation run), and each repetition is indicated in Table 3. An initial distance between grips of 115 mm and a span width of 30 mm were used for tensile and flexural testing, respectively. Both tensile and flexural testings were performed using a mechanical test system 5800R (Instron, High Wycombe, UK), using a cross-head speed of 2 mm/min (tensile) and 1 mm/min (flexural) – determined from the EN ISO 14 125 [**20**] to provide a 1 per cent strain rate. All mechanical tests were performed at 25 °C/50 per cent Rh. The dominant failure modes are shown in Fig. 3 (tensile testing) and Fig. 4 (flexural testing). Most samples failed within the gage, and were acceptable. A number of samples also failed outside the gage and were excluded from subsequent analyses.

## 3 RESULTS

### 3.1 Calculation of mechanical properties

The tensile modulus, $E_t$ (MPa), was calculated from a linear regression fit of the linear region of force ($N$)–extension (mm) plot of the data. Cross-sectional areas were calculated using average measured values of width and thickness of each sample, and were employed in the calculation of $E_t$. The ultimate tensile strength, $U_t$ (MPa), of each sample was calculated from the peak force of the load–extension plot and the calculated sample cross-sectional area. The modulus of elasticity in bending, $E_b$ (MPa), was calculated using the standard equation (equation (1))

$$E_b = \frac{L^3}{4bd^3}\left(\frac{\Delta f}{\Delta s}\right) \tag{1}$$

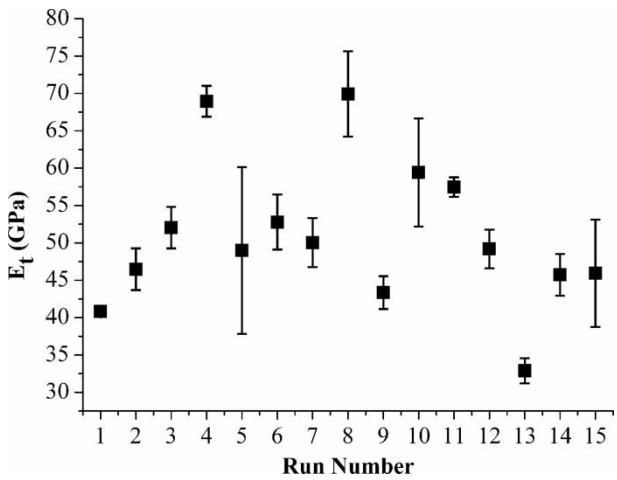


**Fig. 5** Average tensile modulus ($E_t$)

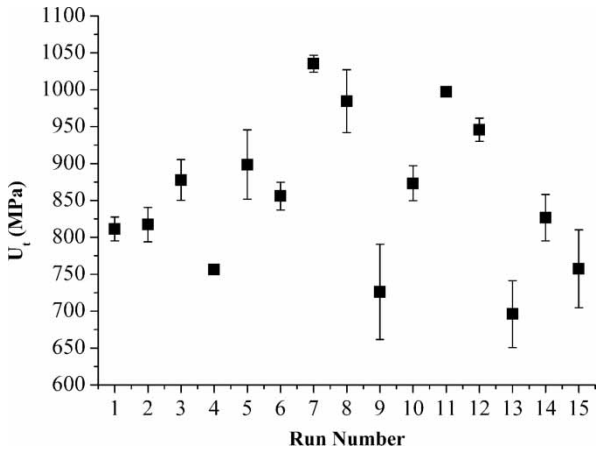


**Fig. 6** Average ultimate tensile strength ($U_t$)

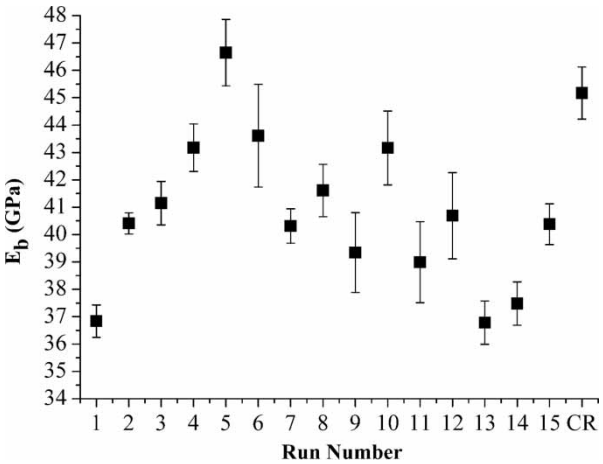


**Fig. 7** Average modulus of elasticity in bending ($E_b$)

where $L$ is the span ($30 \pm 0.3$ mm), $b$ is the sample width (nominal of $25 \pm 0.2$ mm), $d$ is the sample thickness (mm), and $\Delta f = f'' - f'$, where $f'$ and $f''$ are the force at a mid-span displacement $s'$ and $s''$ (calculated for a strain of $\varepsilon_f'$ (0.0005) and $\varepsilon_f''$ (0.0025)) using equation (2)

$$s' = \frac{\varepsilon_f' L^2}{6d} \quad \text{and} \quad s'' = \frac{\varepsilon_f'' L^2}{6d} \tag{2}$$

where $\Delta s = s'' - s'$.

The flexural strength, $\sigma_f$ (MPa), was calculated using the standard equation

$$\sigma_f = \frac{3PL}{2bd^2} \tag{3}$$

where $P$ is the maximum force ($N$) value of the force ($N$)–extension (mm) plot.

The average values for each measured mechanical property of the six samples within each repetition, for each run (including the confirmation run –CR) (average of 36 measurements per run), are presented in Figs 4 to 7.

### 3.2 Statistical analysis of process parameter significance

The significance of the process parameters ($d_i$, $n$, and $v_c$) on the calculated values of $E_t$, $U_t$, $E_b$, and $\sigma_f$ were assessed using a $Y$-hat linear regression of the results of the parameter matrix (Table 1) and an analysis of variance (ANOVA) was performed on the resultant regression tables. The results of the ANOVA analyses for each of the measurables are given in Table 4. A multiple response optimization, based on the $Y$-hat linear regression, was used to optimize individually for each parameter. The optimized process parameters are given in Table 5.

### 3.3 Process capability analysis

A single-sided process capability analysis was performed to assess the robustness of the process. The lower spec limit (LSL) required to deliver a Cpk or 1.25 (existing process) [**21**] and 1.45 (new process) [**21**]

**Table 5** Optimized process parameters for maximum $E_t$, $U_t$, $E_b$, and $\sigma_f$

| | Optimized process parameters | | |
|---|---|---|---|
| Response | $d_i$ (mm) | $n$ | $v_c$ (mm/min) |
| $E_t$ | 8 | 7 | 1.00 |
| $U_t$ | 8 | 8 | 0.46 |
| $E_b$ | 8 | 6 | 0.25 |
| $\sigma_f$ | 8 | 6 | 0.25 |

**Table 4** Results of an ANOVA analysis of the mechanical properties

| | $E_t$ | | | $U_t$ | | | $E_b$ | | | $\sigma_f$ | | |
|---|---|---|---|---|---|---|---|---|---|---|---|---|
| Source | $F$ | $P$ | % | $F$ | $P$ | % | $F$ | $P$ | % | $F$ | $P$ | % |
| $d_i$ | 8.022 | 0.001 | 26.57 | 8.291 | 0.001 | 32.08 | 26.593 | 0.000 | 23.36 | 7.522 | 0.001 | 33.41 |
| $n$ | 8.408 | 0.001 | 10.29 | 0.031 | 0.969 | 0.12 | 2.680 | 0.076 | 2.35 | 1.371 | 0.261 | 6.09 |
| $v_c$ | 4.584 | 0.014 | 0.29 | 1.055 | 0.354 | 4.08 | 4.571 | 0.014 | 4.02 | 0.493 | 0.613 | 2.19 |
| AB | 7.749 | 0.001 | 27.71 | 2.924 | 0.028 | 22.62 | 25.855 | 0.000 | 45.43 | 2.718 | 0.037 | 24.15 |
| AC | 0.186 | 0.945 | 0.85 | 0.076 | 0.989 | 0.59 | 3.981 | 0.006 | 6.99 | 0.368 | 0.831 | 3.27 |
| BC | 0.075 | 0.990 | 2.04 | 0.176 | 0.950 | 1.36 | 0.500 | 0.736 | 0.88 | 0.068 | 0.991 | 0.61 |
| ABC | 1.893 | 0.077 | 19.16 | 3.450 | 0.002 | 53.38 | 3.604 | 0.002 | 12.67 | 3.955 | 0.001 | 70.27 |
| Error | | | 52.25 | | | 121.87 | | | 27.68 | | | 139.93 |

**Table 6** Process capability for the non-optimized and optimized VCT process

| | $E_t$ (GPa) | | $U_t$ (MPa) | | $E_b$ (GPa) | | $\sigma_f$ (MPa) | |
|---|---|---|---|---|---|---|---|---|
| | Existing | New | Existing | New | Existing | New | Existing | New |
| *Non-optimized process* | | | | | | | | |
| LSL | 32.06 | 29.97 | 617.00 | 567.64 | 33.92 | 33.14 | 902.04 | 880.01 |
| $\bar{x}$ | 45.07 | 45.07 | 924.26 | 924.26 | 38.75 | 38.75 | 1039.18 | 1039.18 |
| $\sigma$ | 3.48 | 3.48 | 82.27 | 82.27 | 1.29 | 1.29 | 36.72 | 36.72 |
| Cpk | 1.25 | 1.45 | 1.25 | 1.45 | 1.25 | 1.45 | 1.25 | 1.45 |
| DPM | 93.00 | 7.20 | 93.87 | 7.28 | 93.73 | 7.29 | 93.84 | 7.29 |
| *Optimized process* | | | | | | | | |
| LSL | – | – | – | – | 41.61 | 41.04 | 1104.30 | 1092.62 |
| $\bar{x}$ | – | – | – | – | 45.17 | 45.17 | 1177.00 | 1177.00 |
| $\sigma$ | – | – | – | – | 0.95 | 0.95 | 19.46 | 19.46 |
| Cpk | – | – | – | – | 1.25 | 1.45 | 1.25 | 1.45 |
| DPM | – | – | – | – | 93.73 | 7.32 | 93.73 | 7.27 |

was determined for the non-optimized and optimized system, and the results are given in Table 6.

## 4 DISCUSSION

### 4.1 Tensile modulus ($E_t$)

As expected, there is a wide range of scatter (5.9 per cent) in the values obtained for $E_t$ (Fig. 5), with mean ($\bar{x}$) of $51 \pm 3$ GPa. The ANOVA results (Table 4) indicate that there is a high level of interaction between process parameters, with the AB($d_i$, $n$) and ABC ($d_i$, $n$, $v_c$) interactions having contributions of 27.71 per cent and 19.16 per cent, respectively. This high level of interaction can be assumed to be a result of the mechanical strength being determined by a combination of the fibre content within the resin matrix, the quality of the matrix, and its adhesion to the fibres. The former is determined solely by $n$ (for a fixed thickness component), whereas the latter will be determined by the resistance to resin flow within the cavity, and is likely to be determined by all three parameters. The most significant single contributing parameter was initial mould gap ($d_i$) (26.57 per cent), which has a good signal-to-noise ratio ($F$-ratio of 8.022). The optimization for maximum $E_t$ (Table 5) indicates using a maximum level for $d_i$, suggesting that the resin flow is indeed enhanced by increasing the cavity volume prior to resin infusion. An intermediate number of layers of fabric is predicted, which reflects the strong interaction between $d_i$ and $n$, and suggests that the resin flow is restricted by increasing carbon layers. The optimization demands the highest level for $v_c$, although the significance and $F$-ratio of $v_c$ are low (0.29 per cent, 4.584). Since the resin was restricted to a single exit, higher closure rates induce a higher pressure within the resin, which may encourage more complete resin infusion of the dry fabric. The average value for $E_t$ of $51 \pm 3$ GPa compares favourably against values obtained for similar NCF materials processed using the resin infusion under flexible tooling (RIFT) (48–61 GPa) [**22**] and compression moulding [**23**]. The highest value for $E_t$ of 69.93 GPa is also comparable to those obtained through RTM, where 65–70 GPa is considered the upper end of values obtainable by this process [**22**]. It also compares well against autoclave processing of bi-directional cloth (72 GPa) [**24**] and 57.8–71.5 GPa [**25**], but is significantly lower than values obtained through filament winding (125–145 GPa) [**25**].

### 4.2 Ultimate tensile strength ($U_t$)

The scatter observed in $U_t$ (3.0 per cent) (Fig. 6) was lower than that observed for $E_t$, having $\bar{x}$ of $857 \pm 26$ MPa. Similarly, for $U_t$, the most significant contribution (Table 4) was from the ABC interaction (53.38 per cent), and again, the AB interaction was also highly significant (22.62 per cent). Again, the most significant single parameter was $d_i$ (32.08 per cent, $P = 0.001$), for which again the optimal value was at the maximum level. These results again reinforce the benefit of the variable cavity process methodology on part quality. Surprisingly, the effect of the number of fabric layers in the sample was insignificant (0.12 per cent, $P = 0.969$), suggesting that $U_t$ of the samples manufactured using this process is more dependent on the degree and quality of resin infiltration than on the fibre volume fraction. An intermediate closure rate is demanded by the optimization, but the significance of this factor is very low (4.08 per cent, $P = 0.354$), and the effect of this parameter on $U_t$ is thus small. The highest value obtained for $U_t$ of 1035 MPa (Fig. 5) is significantly higher than those obtained for compression moulded tri-axial woven carbon fabric (220–500 MPa) [**24**], and for RIFT (600–800 MPa) [**22**], and are comparable to the highest values obtainable for RTM (830 MPa) [**23**]. The average $U_t$ of $857 \pm 26$ MPa also compares reasonably favourably with results obtained for autoclave-moulded (0/90°) composite (810–1185 MPa) [**26**]. It should be noted that these comparisons are not absolute, as in each

case, the testing method and/or materials were different to those employed in this study. The low $U_t$ obtained for compression moulded tri-axial fibres in reference [**24**] was concluded to be due to breakage of 0° fibres, underlying the impact of fibre type and orientation on mechanical test results.

### 4.3 Modulus of elasticity in bending ($E_b$)

The scatter in $E_b$ ($\bar{x} = 40.7 \pm 0.7$ GPa) (Fig. 7) of (1.7 per cent) is lower than that observed in the values for $E_t$ and $U_t$. The most significant parameter is $d_i$–23.36 per cent ($F$-ratio of 26.59 per cent, $P < 0.3$ dp) (Table 4), which again is predicted to be at the maximum level of 8 mm for the optimized system (Table 5). Surprisingly, the optimized $n$ value is at its minimum level (six fabric layers); however, even though $n$ and $v_c$ are both statistically significant ($P > 0.05$), their contribution to $E_b$ is small (2.35 per cent and 4.02 per cent respectively), and it can again be proposed that variation of process parameters has a more significant effect on the level and quality of the resin matrix, which is more important in determining $E_b$ (in this process) than the volume fraction of carbon within the structure. The average value obtained ($40.7 \pm 0.7$ GPa) for the non-optimized process is commensurate with the upper levels expected from a vacuum-assisted resin infusion moulding (VARIM) process (35–40 GPa) [**27**], but underperforms relative to autoclave processing (42.1–49.3 GPa) [**28**] and RTM (44 GPa) [**28**]. The upper value obtained through the non-optimized process ($47 \pm 1$ GPa) (Fig. 5) exceeds the level obtained through VARIM [**26**] and RTM [**29**] and is in alignment with values observed for autoclave processing [**28**]. The optimized value $45 \pm 1$ GPa (Run CR of Fig. 7) is statistically comparable to the highest value obtained for the non-optimized system. This is to be expected since the optimized process parameters for this part ($d_i = 8$, $n = 6$, $v_c = 0.25$) (Table 5) are the same as those employed in Run 5 (Table 3) to manufacture the best performing non-optimized sample.

### 4.4 Flexural strength ($\sigma_f$)

The scatter observed in $\sigma_f$ ($\bar{x} = 1109 \pm 15$ MPa) (1.35 per cent) (Fig. 8) is the lowest of all the measured responses. The interaction ABC dominates the ANOVA results (Table 4), with a contribution of 70.27 per cent, which again demonstrates the complexity of the process, and the need for a statistical analysis. Again, as for $E_b$, the process parameter presenting the largest contribution to variation in $\sigma_f$ is $d_i$ – 33.41 per cent) ($F$-ratio of 7.52, $P < 03$ dp). Although there is a very large ABC interaction, B and C show no individual statistical significance, with $P \gg 0.05$ for both $n$ and $v_c$ (Table 4). As for $E_b$, the level and quality of the resin matrix is more important in determining

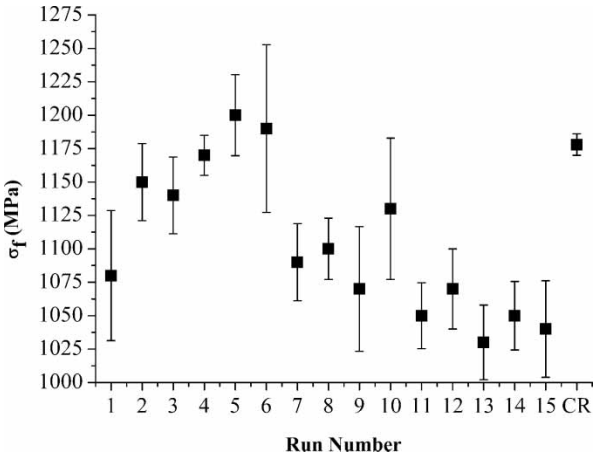


**Fig. 8** Average flexural strength ($\sigma_f$)

$\sigma_f$ than the volume fraction of carbon within the structure (in this process). The non-optimized $\sigma_f$ ($\bar{x} = 1109 \pm 15$ MPa) is significantly higher (order of three times) than the previous values observed for VARIM [**27**], and approximately double those observed for RTM ($536 \pm 40$ MPa) [**29**]. The average and maximum ($1170 \pm 30$) non-optimized values fall short of autoclave-processed materials (1350–1900 MPa) [**28**], $1923 \pm 39$ MPa [**30**], which is not unexpected, since pressures of 0.7 MPa are employed in the prior studies, and only 0.1 MPa was employed in this study. The optimized $\sigma_f$ of $1177 \pm 8$ MPa (Run CR of Fig. 6) is an improvement over the non-optimized values but still falls short of autoclave levels.

### 4.5 Process capability (Cpk)

Cpk is an indication of how well a process performs (i.e. how the mean and standard deviation conforms to the production requirements). A Cpk of 1.25 is considered representative of that expected from an existing process, and represents approximately 93 defects per million (DPM) [**21**]. A more stringent requirement is a Cpk of 1.45, which is expected of a new process, and represents only 7 DPM [**21**]. Table 6 indicates the LSL required to achieve each of these criteria. An LSL is the lowest value that could result from the process. A wider acceptance limit (and thus a lower LSL) provides a higher Cpk. From Table 6, it is clear that the process is not very capable. For a Cpk of 1.45, the predicted LSL for both $E_t$ and $U_t$ is below that expected from either the VARIM or RTM processes. Only when Cpk is relaxed to 1.25 is the LSL for $U_t$ comparable to VARIM quality. For the flexural properties, the capability is slightly improved, with $\sigma_f$ for the LSL being comparable to VARIM and RTM quality, although $E_b$ results are still poor, with no values $E_b$ for the LSL being comparable to standard processes. Optimization of the process for the flexural properties does provide some improvement in the capability for both $E_b$ and $\sigma_f$, bringing the

LSL values for $\sigma_f$ for both 1.25 and 1.45 Cpk up and placing the process at a competitive level to the VARIM and RTM processes. The lack of process capability is likely to be due to the manual nature of the process. All carbon fibre laminate cutting was performed manually and resin injection was also manually controlled. Automation of the process would be expected to significantly improve the capability of the process, raising the LSL.

Although automation is suggested, this will affect the cost-effectiveness of the process. In this case, however, only 'simple' automation is implied, such as the inclusion of automated control over resin infusion time and pressure, and automated cutting of the laminates. These steps are not deemed to be out of the norm for an industrial context, but they represent a significant improvement over the manual practices in this research and are thus likely to significantly improve process capability at minimal increased cost. This in turn will offer cost savings in terms of reduced scrap rates and reduced material usage.

Many other variables of type 1 (controllable and measurable), type 2 (measurable but not controllable), and type 3 (non-measurable and uncontrollable) may also affect the measured response of the system; but within the resources of the project, only a limited number of factors could be analysed using full factorial experiment. A partial factorial experiment was considered, which would have allowed the number of factors to be extended, but it was considered that interactions between the main parameters (two-way) may be important (and were indeed seen to be so—Table 4), and thus a full factorial approach was employed. Further studies will be required to evaluate other parameters (such as injection pressure), and a designed experiment incorporating the statistically important factors so far identified and new factors.

### 4.6 Process cost

As previously mentioned, although the aim of this article is not to provide a cost analysis of the process, potential sources of likely cost savings may be presented. Fundamentally, the ability to infuse dry fabric at low injection pressures (0.1 MPa) allows the use of low-cost tooling materials. The costs savings achievable through substitution of tool steels with aluminium may not be great, and indeed, aluminium may be more expensive than tool steels, but cost savings may be achieved in the machining of the aluminium, since significant savings in cutting times can be achieved using aluminium over tool steel (3–10 times shorter cutting times), resulting in up to 30 per cent reduction in tool costs [**31**], thus, over an entire UAV, with perhaps 200 moulded parts, the cost savings can be substantial. Even more savings may be possible through the use of non-conventional tooling materials, including polymers. A recent review of tooling materials for composites [**32**] suggested that a significant cost saving may be achieved through the use of net-shape cast polymeric tooling, such as a cast resin or metal spray tooling inserts. These are sufficiently durable to withstand the low injection pressures used in this process. Cost savings of 50 per cent in material costs, and removal of almost all machining costs (some minor machining may be required for finishing of inserts), may be achieved with the use of these materials.

## 5 CONCLUSIONS

The variable cavity process has been shown to provide components having tensile and flexural properties that compare very favourably with those obtained for RTM-processed components.

The interaction between the three primary processing parameters is highly significant, but the overwhelming contribution to the level of the observable responses was found to be due to the initial mould gap ($d_i$). The contribution of the two other parameters was low in all cases, indicating that the improvement in resin flow and infusion quality was primarily determined by $d_i$ and was largely independent of the volume fraction of carbon in the final component (within the range used for the parameters).

This has demonstrated that high-quality resin infusion at low pressure (0.1 MPa) can be achieved by introducing a larger cavity during the infusion stage of the VARTM process. This allows lower-cost materials to be used for the tooling (e.g. aluminium and potentially tooling grade cast resins, etc.).

Process optimization was valuable in improving the capability of the process but further process refinement is required, primarily through increased process automation, to further increase the capability. Further investigation of the process is required to enable full optimization. In particular, the tool specification restricted the range of the parameters, particularly $n$, the number of fabric layers. A higher closing force would be required to increase $n$ above 8, but this would be highly desirable since the volume of the fibre in the cavity at higher levels may become more critical in determining part quality.

## ACKNOWLEDGEMENTS

The research was co-funded by the FLAVIIR research grant from the Engineering and Physical Sciences Council (EPSRC) (FLAVIIR is a funding collaboration between the EPSRC and BAE Systems) and the Warwick Innovative Manufacturing Research Centre (WIMRC), an EPSRC-funded initiative.

## REFERENCES


1 **Achim, V., Soukane, S., Trochu, F.,** and **Bréard, J.** Optimization of injection flow rate to minimize micro/macro-voids formation in resin transfer molded composites. *Compos. Sci. Technol.*, 2006, **66**(3–4), 475–486.

2 **Bowles, K. J.** and **Frimpong, S.** Void effects on the interlaminar shear strength of unidirectional graphite-fiber-reinforced composites. *J. Compos. Mater.*, 1992, **26**(10), 1487–1509.

3 **Armstrong, D. L., Goodwin, S. L., Sharpless, G., Hethcock, J. D., Andrews, J.,** and **Coyle, L.** Development of a low-cost integrated RTM horizontal stabilizer that flies on Bell Helicopter's MAPL. *SAMPE J.*, 2006, **42**(3), 54–62.

4 **Sutton, G.** Affordable RTM aerospace components. *SAMPE J.*, 1999, **35**(3), 58–63.

5 **Cochran, R., Matson, C., Thoman, S.,** and **Wong, D.** Advanced composite processes for aerospace applications. In Proceedings of the International SAMPE Symposium and Exhibition on Evolving Technologies for the Competitive Edge, Anaheim, California, USA, 1997, vol. 42, no.1, pp. 635–640.

6 **Toi, Y., Harada, A., Tanaka, S., Amaoka, K.,** and **Kikukawa, H.** Development of affordable composite wing structure. *Adv. Compos. Mater.: Off. J. Jpn. Soc. Compos. Mater.*, 2004, **12**(4), 321–329.

7 **Backhouse, R.** Mercedes Benz SLR McLaren – a step towards affordable CFRP structures. In Proceedings of the Sixth Annual SPE Automotive Composites Conference, Detroit, Michigan, USA, 2006, p. 859.

8 **Grande, J.** One step to processed auto parts. *Mod. Plast. Int.*, 1995, **25**(5), 52.

9 **Cairns, D. S.** and **Skramstad, J. D.** Evaluation of hand lay-up and resin transfer molding in composite wind turbine blade structures. In Proceedings of the International SAMPE Symposium and Exhibition, Long Beach, California, USA, 2000, vol. 45, no. I, pp. 967–980.

10 **Ikegawa, N., Hamada, H.,** and **Maekawa, Z.** Effect of compression process on void behavior in structural resin transfer molding. *Polym. Engng Sci.*, 1996, **36**(7), 953–962.

11 **Choi, J. H.** and **Dharan, C. K. H.** Enhancement of resin transfer molding using articulated tooling. *Polym. Compos.*, 2002, **23**(4), 674–681.

12 **McConnell, V. P.** Advanced RTM produces complex, repeatable, flight-critical parts. *SAMPE J.*, 1998, **34**(6), 37–43.

13 **Shojaei, A.** Numerical simulation of three-dimensional flow and analysis of filling process in compression resin transfer moulding. *Compos. Part A, Appl. Sci. Manuf.*, 2006, **37**(9), 1434–1450.

14 **Plessinger, J., Myers, J., Brachos, V.,** and **Rossi, G.** Development of a sequential multiport resin injection manifold system (SMRIMS) to RTM a 16 ft structural car chassis. In Proceedings of the International SAMPE Technical Conference, Covina, California, USA, 1998, vol. 30, pp. 361–372.

15 **Babu, B. J. C., Prabhakaran, R. T. D.,** and **Agrawal, V. P.** Quality evaluation of resin transfer molded products. *J. Reinf. Plast. Compos.*, 2008, **27**(6), 559–581.

16 **Seeman, W. H.** *Plastic transfer molding techniques for the production of fiber reinforced plastic structures*. US Patent 4902215, 1990.

17 **Brouwer, W. D., Van Herpt, E. C. F. C.,** and **Labordus, M.** Vacuum injection moulding for large structural applications. *Compos. Part A, Appl. Sci. Manuf.*, 2003, **34**(6), 551–558.

18 **Sewell, T. A., Wanthal, S.,** and **Rapp, R.** Improved laminate physical and mechanical properties using 'hytest' vacuum assisted resin transfer molding. In Proceedings of the International SAMPE Symposium and Exhibition, Long Beach, California, USA, 2005, vol. 50, pp. 1271–1287.

19 British Standards Institute. Plastics – determination of tensile properties. Part 4: test conditions for isotropic and orthotropic fibre-reinforced plastic composites. BS EN ISO 527-4,1997.

20 British Standards Institute. Fibre-reinforced plastic composites – determination of flexural properties. BS EN ISO 14125,1998.

21 **Montgomery, D.** *Introduction to statistical quality control*, 2005, p. 776 (John Wiley, New York).

22 **Mills, A.** AMICC project laminate characterisation. Internal AMICC Project Report, Centre for Lightweight Composites, Cranfield University, 2001.

23 Anon. RTM 120/HY2954. 120C Epoxy System for RTM Product Data Sheet. Hexcel Composites ITA 086, 1998.

24 **Fujita, A., Hamada, H.,** and **Maekawa, Z.** Tensile properties of carbon fibre triaxial woven fabric composites. *J. Compos. Mater.*, 1993, 1428–1442.

25 **Schwartz, M. M.** *Composite materials handbook*, 1992 (McGraw-Hill, London).

26 **de Paiva, J. M. F., Mayer, S.,** and **Rezende, M. C.** Comparison of tensile strength of different carbon fabric reinforced epoxy composites. *Mater. Res.*, 2006, **9**(1), 83–89.

27 **Chowdhury, F. H., Hosur, M. V.,** and **Jeelani, S.** Studies on the flexural and thermomechanical properties of woven carbon/nanoclay-epoxy laminates. *Mater. Sci. Eng.*, 1989, **421**(1–2), 298–306.

28 **Tarpani, J. R., Milan, M. T., Spinelli, D.,** and **Bose, W. V.** Mechanical performance of carbon-epoxy laminates. Part I: quasi-static and impact bending properties. *Mater. Res.*, 2006, **9**(2), 115–120.

29 **Papargyris, D. A., Day, R. J., Nesbitt, A.,** and **Bakavos, B.** Comparison of the mechanical and physical properties of a carbon fibre epoxy composite manufactured by resin transfer moulding using conventional and microwave heating. *Compos. Sci. Technol.*, 2008, **68**, 1854–1861.

30 **Davies, L. W., Day, R. J., Bond, D., Nesbitt, A., Ellis, J.,** and **Gardon, E.** Effect of cure cycle heat transfer rates on the physical and mechanical properties of an epoxy matrix composite. *Compos. Sci. Technol.*, 2007, **67**, 1892–1899.

31 **Hunt, W.,** and **Skillingberg, M.** Specialized aluminium products for tool and mold applications. *Aluminum Now*, 2004, May/June, 23–24.

32 **Gibbons, G. J., Hansell, R. G., Thacker, G.,** and **Arnett, G.** State of the art in low-cost, rapid composite forming tooling technologies. *J. Adv. Mater.*, 2009, **41**(2), 5–19.

## APPENDIX

### Notation

| | |
|---|---|
| $b$ | sample width used in measuring $E_b$ |
| $d$ | sample thickness used in measuring $E_b$ |
| $d_f$ | final mould gap |
| $d_i$ | initial mould gap |
| $E_b$ | modulus of elasticity in bending |
| $E_t$ | tensile modulus |
| $f'$ | force at a mid-span displacement $s'$ (calculated for a strain of $\varepsilon'_f = 0.0005$) |
| $f''$ | force at a mid-span displacement $s''$ (calculated for a strain of $\varepsilon'_f = 0.0025$) |
| $L$ | sample span used in measuring $E_b$ |
| $n$ | number of CFC fabric layers |
| $P$ | maximum force ($N$) value of the force ($N$)–extension (mm) plot for flexural testing |
| $P_c$ | closure pressure |
| $P_{i1}$ | resin injection pressure |
| $P_{i2}$ | resin injection pressure |
| $P_{v1}$ | vacuum pressure |
| $P_{v2}$ | vacuum pressure during resin injection |
| $t_c$ | closure time |
| $t_{i1}$ | time of application of resin injection pressure |
| $t_{i2}$ | time of application of resin injection pressure after mould closure |
| $t_o$ | initial time |
| $t_{v1}$ | application time of $P_{v1}$ |
| $U_t$ | ultimate tensile strength |
| $v_c$ | mould cavity closure rate |
| $V_{i1}$ | resin volume |
| $\Delta f$ | $f''$-$f'$ |
| $\Delta s$ | $s'' - s'$ |
| $\varepsilon'_f$ | flexural strain of 0.0005 |
| $\varepsilon''_f$ | flexural strain of 0.0025 |
| $\sigma_f$ | flexural strength |